

NJC

Accepted Manuscript



This is an *Accepted Manuscript*, which has been through the Royal Society of Chemistry peer review process and has been accepted for publication.

Accepted Manuscripts are published online shortly after acceptance, before technical editing, formatting and proof reading. Using this free service, authors can make their results available to the community, in citable form, before we publish the edited article. We will replace this *Accepted Manuscript* with the edited and formatted *Advance Article* as soon as it is available.

You can find more information about *Accepted Manuscripts* in the [Information for Authors](#).

Please note that technical editing may introduce minor changes to the text and/or graphics, which may alter content. The journal's standard [Terms & Conditions](#) and the [Ethical guidelines](#) still apply. In no event shall the Royal Society of Chemistry be held responsible for any errors or omissions in this *Accepted Manuscript* or any consequences arising from the use of any information it contains.

Cite this: DOI: 10.1039/c0xx00000x

www.rsc.org/xxxxxx

ARTICLE TYPE

Rare intermolecular M \cdots H-C anagostic interactions in homoleptic Ni(II) / Pd(II) dithiocarbamate complexes

Manoj Kumar Yadav^a, Gunjan Rajput^a, Lal Bahadur Prasad^a, Michael G. B. Drew^b and Nanhai Singh^{*a}

Received (in XXX, XXX) Xth XXXXXXXXX 20XX, Accepted Xth XXXXXXXXX 20XX

DOI: 10.1039/b000000x

New functionalized homoleptic dithiocarbamates of the form [M(L)₂] (M= Ni(II), L= **L1**, *N*-(3-methoxybenzyl)-*N*-(methylbenzyl)dithiocarbamate (**1**), **L3**, *N*-(3,4,5-trimethoxybenzyl)-*N*-(3-methylpyridyl)dithiocarbamate (**3**), **L4**, *N*-(4-methoxybenzyl)-*N*-benzylidithiocarbamate (**4**); Pd(II), **L2**, *N*-(*N'*-methyl-2-pyrrole)-*N*-benzylidithiocarbamate (**2**)) have been synthesized and characterized by microanalysis and their structures have been investigated by X-ray crystallography. The four structures are all centrosymmetric with the metal located in a square plane with minor distortions, Pd(II) greater than Ni(II). The crystal structures of **1** and **2** revealed the existence of unique intermolecular C–H \cdots M (Ni, Pd) anagostic interactions between the methylene hydrogen atom on the ligand substituents and the metal centres and these enable the formation of 1-D polymeric chains. Particularly geometric parameters (Pd \cdots H–C = 2.61 Å; \angle Pd \cdots H–C = 173°) for the C–H \cdots Pd interactions in **2** are at the border of anagostic and hydrogen bonding. By contrast, **4** shows interactions between the methylene hydrogen and the CS₂Ni ring rather than the metal alone, while the interaction in **3** is intermediate between the two aforementioned types. These interactions are not retained in solution as revealed by their ¹H NMR studies. DFT calculations have been performed to analyse these rare interactions. **1**, **3** and **4** are weakly conducting, σ_{rt} = 10⁻¹⁰-10⁻¹² S cm⁻¹ and show semiconductor behaviour in the 313-373 K range.

Introduction

Metal dithiocarbamate complexes have been widely studied because of their rich diversity of structures, interesting conducting, magnetic and optical properties, as photosensitizers in solar energy conversion processes, single source MOCVD precursor for the preparation of metal sulphides and nano particles and wide ranging applications.¹⁻⁷ A resurgence of interest in the dithiocarbamate complexes arises due to the functionalisation of substituents on the N atom of the dithiocarbamate backbone that may provide structural scaffolds for novel molecular architectures and modify their chemical reactivity and physical properties.¹⁻⁶ Crystal engineering of metal directed self assembly of coordination compounds afforded by S \cdots H, O \cdots H, N \cdots H, S \cdots S and C–H \cdots π (chelate, CS₂M) secondary interactions play key roles in organization of supramolecular networks.⁸⁻¹⁰

The existence of important C–H \cdots M bonding interactions between the C–H hydrogen atom on the ligand fragment and metal centres providing agostic, anagostic or preagostic and hydrogen bonding interactions are less commonly observed in the organometallic complexes.¹⁰ As compared to agostic bonding, the nature of anagostic and hydrogen bonding interactions have been less explored in the literature. In fact the agostic interactions comprising of 3c-2e bonds are the strongest and supported by a noticeable upfield chemical shift of the participating protons. By comparison, somewhat weaker anagostic interactions are largely

electrostatic in nature and exhibit a downfield shift of the uncoordinated C–H protons.¹⁰ The agostic interactions are stabilised by the electron deficient early transition metals whereas the anagostic interactions are typically associated by d⁸ or even d⁹ metal ions.^{10,11} The agostic and anagostic interactions are characterized by the M \cdots H–C distances of ~ 1.8-2.3 and 2.3-2.9 Å and \angle M \cdots H–C angles of ~ 90-140° and 110-170° respectively. In hydrogen bonding the late electron rich transition metals, Pt(II) and Au(III), have served as proton acceptors¹² forming 3c-4e bond involving X–H \cdots M type interactions where X is an electro negative atom such as nitrogen and oxygen. Such classical hydrogen bonds are nearly linear and accompanied with a downfield shift of the non bonded proton. The C–H bonds in the ligand fragment are believed to be weak hydrogen bond donors because of the relatively lower electronegativity of the carbon atom but are rarely involved in the metal assisted nonconventional intramolecular M–C \cdots H hydrogen bond formation.^{11a} However, it appears that the polar C–H bonds may be substantially engaged in the C–H \cdots M anagostic / hydrogen bonding interactions. In spite of the aid of advanced quantum chemical calculations, in comparison to agostic interactions there is relatively scant evidence regarding structural characteristics i.e. geometrical parameters and optimum C–H \cdots M bond lengths and bond angles for the anagostic and H-bonding interactions.

These metal mediated interactions are of significant importance due to their possible implications in the C–H bond activation. Considerable attention has been devoted to explore the

origin and nature of the anagostic / hydrogen bonding interactions with the aid of spectroscopic techniques, crystallography and theoretical studies.^{10f-h}

The manifestation of multifaceted chemistry of dithiocarbamate complexes may be ascribed to the resonance structures (Fig.1) that this ligand provides in the complexes.

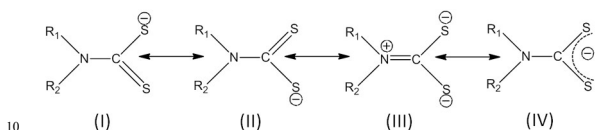


Fig. 1 Resonance structures of the dithiocarbamate ligand.

In recent years we and other groups have reported the existence of intra- and intermolecular anagostic interactions in some homo- and heteroleptic group 10 metal dithiocarbamate complexes.^{6e-j} Influenced by these observations and lack of examples with its nickel congener, Pd it was considered promising to undertake the synthesis, structural investigation and conducting properties of new functionalized Ni(II) and Pd(II) dithiocarbamate complexes. The anagostic and borderline case of anagostic-hydrogen bonding interactions observed in the nickel (1) and palladium (2) complexes respectively have been discussed and their nature has been supported by DFT calculations.

Experimental section

Materials and methods

All reactions were carried out in open under ambient conditions. Reagent grade chemicals and solvents were obtained from commercial sources. The solvents were purified by standard procedures. Potassium salt of the ligands (Fig. 2), N-(3-methoxybenzyl)-N-(methylbenzyl)dithiocarbamate (KL1), N-(N'-methyl-2-pyrrole)-N-benzylidithiocarbamate (KL2), N-(3,4,5-trimethoxybenzyl)-N-(3-methylpyridyl)dithiocarbamate (KL3) and N-(4-methoxybenzyl)-N-benzylidithiocarbamate (KL4) were prepared according to literature procedures by the reaction of appropriate secondary amines with CS₂ and KOH. The experimental details pertaining to melting point, elemental analysis, recording of IR, ¹H and ¹³C{¹H} NMR and UV-Vis. spectra and the measurement of pressed pellet electrical conductivity are the same as described earlier.^{6a-d}

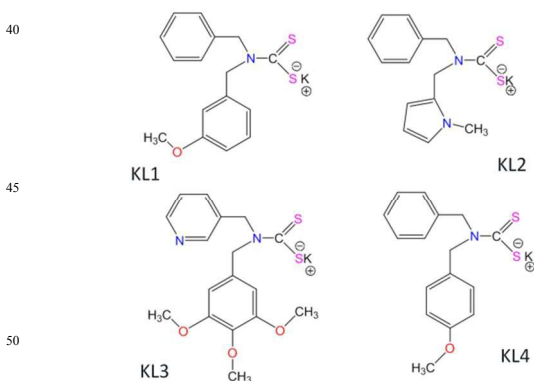


Fig. 2 Structures of the potassium salt of dithiocarbamate ligands used in this work.

Synthesis and characterization of complexes

[M(L)₂] (M=Ni(II), L=L1 (1), L3 (3), L4 (4); Pd(II), L=L2 (2))
 The homoleptic complexes [M(L)₂] were prepared adopting the general procedure. To a 10 mL stirred methanol–water (60:40, v/v) solution of KL1 (0.341, 1 mmol), KL2 (0.330, 1 mmol), KL3 (0.401, 1 mmol) or KL4 (0.341, 1 mmol) was added separately a (5 mL) solution of NiCl₂·6H₂O (0.118 g, 0.5 mmol)/ K₂PdCl₄ (0.163 g, 0.5 mmol) in the same solvent mixture. In each case the reaction mixture was additionally stirred for 4-6 h. The orange-red to dark brown solid products thus formed were filtered off and washed with methanol followed by diethyl ether. The compounds were recrystallized in dichloromethane.
 [Ni(L1)₂] (1): Yield: (76%, 0.252 g), m.p. 154-156°C. Anal. Calcd. for C₃₂H₃₂N₂NiO₂S₄ (663.55): C 57.92, H 4.86, N 4.22 %. Found: C 57.61, H 4.97, N 4.13 %. IR (KBr, cm⁻¹) 1476 (ν_{C-N}), 1000 (ν_{C-S}), ¹H NMR (300.40 MHz, CDCl₃): δ 3.83 (s, 3H, -OCH₃), 4.72 (s, 2H, -CH₂C₆H₅), 4.67 (s, 2H, -CH₂C₆H₄OCH₃), 7.73, 7.71 (m, 2H, -C₆H₄(OCH₃)), 7.32-6.89 (m, 7H, Ar-H) ppm. ¹³C{¹H} NMR (75.45 MHz, CDCl₃): δ 210.08 (-CS₂), 160.16 (Bz-C-OCH₃), 136.17, 134.88, 130.20, 123.97-120.58, 114.00, 113.94 (Ar-C), 55.37 (-OCH₃), 50.86 (-CH₂C₆H₅), 48.13 (-CH₂C₆H₅OCH₃) ppm. UV-Vis. (CH₂Cl₂, λ_{max}(nm), ε (M⁻¹cm⁻¹)): 247 (9.4 x 10⁴), 327 (9.2 x 10⁴), 402.3 (1.6 x 10⁴), 632 (121); σ_π= 0.159 x 10⁻¹⁰ S cm⁻¹
 [Pd(L2)₂] (2): Yield: (87%, 0.285 g), m.p.174-176°C, Anal. Calcd. for C₂₉H₂₉N₃PdS₄ (654.19): C 51.17, H 4.60, N 9.52%. Found: C 50.76, H 4.68, N 8.35 %. IR (KBr, cm⁻¹): 1482 (ν_{C-N}), 978 (ν_{C-S}). ¹H NMR (300.40 MHz, CDCl₃) δ 3.53 (s, 3H, -CH₃), 4.81 (s, 2H, -CH₂-C₄H₃NCH₃), 4.78 (s, 2H, -CH₂-C₆H₅), 6.11, 6.09, 6.07 (m, 3H, -C₄H₃NCH₃), 7.35-6.62 (m, 5H, -C₆H₅) ppm. ¹³C{¹H} NMR (75.45 MHz, CDCl₃) δ 211.89 (-CS₂), 134.05, 133.92, 128.99-128.17, 124.34, 123.31, 112.64 (Ar-C), 50.94 (-CH₂C₆H₅), 43.29 (-CH₂C₄H₃NCH₃), 34.46 (-NCH₃) ppm. UV-Vis. (CH₂Cl₂, λ_{max}(nm), ε (M⁻¹cm⁻¹)): 240 (4.0 x 10⁴), 307 (1.15 x 10⁴), 354 (1.5 x 10⁴), 450 (1.30 x 10³).
 [Ni(L3)₂] (3): Yield: (81%, 0.318 g), m. p. 157-159°C, Anal. Calcd. for C₃₄H₃₈N₄NiO₆S₄ (785.63): C 51.98, H 4.88, N 7.13 %. Found: C 51.62, H 4.97, N 7.02 %. IR (KBr, cm⁻¹): 1464 (ν_{C-N}), 995 (ν_{C-S}). ¹H NMR (300.40 MHz, CDCl₃), δ 3.88 (s, 9H, -OCH₃), 4.64 (s, 2H, -CH₂-C₆H₂ (OCH₃)₃), 4.74 (s, 2H, -CH₂-C₆H₅N), 8.61, 8.50 (m, 2H, -C₆H₅N), 7.73-6.45 (m, 4H, Ar-H) ppm. ¹³C{¹H} NMR (75.45 MHz, CDCl₃) δ 210.01 (CS₂), 153.74 (*meta*, C-C₅H₂(OCH₃)₃), 149.94, 149.59 (C₅H₄N), 138.20 (*para*, C-C₅H₂(OCH₃)₃), 136.10, 128.85, 123.97, 105.53 (Ar-C), 60.89 (*para*, -OCH₃), 56.34 (*meta*, -OCH₃), 51.30 (-CH₂-C₆H₂(OCH₃)₃), 48.15 (-CH₂-C₆H₅) ppm. UV-Vis. (CH₂Cl₂, λ_{max}(nm), ε (M⁻¹cm⁻¹)): 243 (1.93 x 10⁵), 330 (1.62 x 10⁵), 400 (3.05 x 10⁴), 632 (167). σ_π= 0.212 x 10⁻¹¹ S cm⁻¹.
 [Ni(L4)₂] (4): Yield: (74%, 0.245 g), m. p. 160-162°C. Anal. Calcd for C₃₂H₃₂N₂NiO₂S₄ (663.55): C 57.92, H 4.86, N 4.22 %. Found: C 57.63, H 4.91, N 4.15 %. IR (KBr, cm⁻¹) 1488 (ν_{C-N}), 1013 (ν_{C-S}). ¹H NMR (300.40 MHz, CDCl₃), δ 3.83 (s, 3H, -OCH₃), 4.70 (s, 2H, -CH₂-C₆H₄OCH₃), 4.66 (s, 2H, -CH₂-C₆H₅), 6.88 (m, 2-*meta*-H, -C₆H₄OCH₃), 7.38-7.25 (m, 7H, Ar-H) ppm. ¹³C{¹H} NMR (75.45 MHz, CDCl₃) δ 201.16 (CS₂), 158.08 (*para* C, -C₆H₄OCH₃), 132.77, 132.07, 130.57, 128.84 (Ar-C), 59.46 (-OCH₃), 45.01 (-CH₂-C₆H₄OCH₃), 44.32 (-CH₂-C₆H₅) ppm. UV-Vis. (CH₂Cl₂, λ_{max}(nm), ε (M⁻¹cm⁻¹)): 245 (8.23 x 10⁴), 329 (7.86

Cite this: DOI: 10.1039/c0xx00000x

www.rsc.org/xxxxxx

ARTICLE TYPE

x 10⁴), 400 (1.45 x 10⁴), 635 (114). $\sigma_{\text{H}} = 0.464 \times 10^{-12} \text{ S cm}^{-1}$.**X-ray structure determinations**

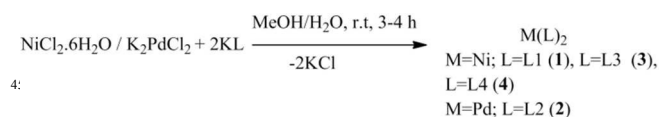
Single crystals of the complexes **1-4** were grown by slow evaporation of the solution of products in CH₂Cl₂. The X-ray diffraction data were collected on an Oxford X-calibur CCD diffractometer using Mo K α radiation with **1**, **3** and **4** at 293(2) K and **2** at 150(2) K. Data reductions were carried out using the CrysAlis program.¹³ The structures were solved by direct methods using SHELXS-97¹⁴ and refined on F² by full matrix least squares method using SHELXL-97.¹⁴ Non-hydrogen atoms were refined anisotropically and hydrogen atoms were geometrically fixed with displacement parameters equivalent to 1.2 times that of the atom to which they were bonded. The -OMe group in **1** was disordered over two sites in different aromatic rings. Populations were set at x and 1-x with x refining to 0.52(1). In **2** one ring in the ligand was disordered between N-methyl-2-pyrrole and phenyl and both options were given a population of 0.50. Diagrams for all complexes were prepared using ORTEP¹⁵ and Mercury software.

Theoretical calculations

All calculations were carried out using the Gaussian 03 program.¹⁶ Structures were optimized using the B3LYP density functional together with basis sets LANL2DZ for Ni, Pd; 6-31+G* for S and 6-31G for the remaining atoms. Starting models were taken from the crystal structures with disorder removed but with hydrogen atoms given theoretical positions. Single point calculations were carried out on models of structures **1** and **2** using one and three molecules (Fig. 6).

Results and discussion**Synthesis and spectroscopy**

The homoleptic complexes **1-4** were isolated in good yield by metathesis reactions of an aqueous-methanolic solution of the metal salts and potassium salt of the ligands (KL1–KL4, Scheme 1, Fig. 2) in 1:2 molar ratios. All complexes are stable to air and moisture and melt in the 154–176°C temperature range. The complexes have been characterized by microanalysis and their structures have been investigated by X-ray crystallography; **1** and **2** show intermolecular C–H...Ni / Pd anagostic interactions while **4** shows interactions between methylene hydrogen atom and the CS₂Ni ring while the interaction in **3** is intermediate between the two aforementioned types. The pressed pellet conductivity of **1**, **3** and **4** has been studied.

Scheme 1. General methodology for the synthesis of complexes **1-4**.

All the complexes show $\nu_{\text{(C-N)}}$ and $\nu_{\text{(C-S)}}$ vibrations at 1464-1488 and 995-1013 cm⁻¹ characteristic of coordinated dithiocarbamate ligands. A significant enhancement in the $\nu_{\text{(C-N)}}$ frequency of the complexes in comparison to free dithiocarbamate ligands (160-193 cm⁻¹) indicates the dominant contribution of the canonical form (IV), Fig. 1. ¹H NMR of all the complexes exhibit resonances characteristic of the ligand functionalities and integrate well to the corresponding protons. The ¹H NMR of **1-4** show downfield shifting in δ 4.64-4.81 ppm region for the methylene hydrogen atoms due to metal-dithiocarbamate ligand coordination. Two close singlets are observed for these protons on each ligand functionality with a difference in peak position of δ 0.03-0.10 ppm. To confirm the existence of anagostic interactions observed in the crystal structure of **1** (*vide infra*) the low temperature proton NMR study was carried out down to liquid nitrogen temperature which could not reveal a significant down field shift of the uncoordinated proton thereby confirming that the intermolecular C–H...M interactions are not retained in solution. This kind of difference between the solid state and solution structures in the case of intramolecular C–H...M hydrogen bonding is known.^{11a-b} The intermolecular C–H...M interactions are rare and are generally not retained in solution but are stabilized in the solid state. In the ¹³C NMR an upfield shift of δ 5-15 ppm for the NCS₂ carbon in the complexes (δ 201–211 ppm) as compared to uncoordinated ligands (δ 215-216 ppm) is indicative of metal-ligand bonding.

Crystal Structures

The single crystals of **1-4** were obtained by slow evaporation of the solution of compounds in dichloromethane. Selected bond angles and bond lengths and crystallographic parameters are listed in Tables 1 and 3 respectively. The metal atoms occupy a crystallographic centre of symmetry in all the complexes, thus each asymmetric unit contains half a discrete molecule. Their ORTEP representations are shown in Fig. 3.

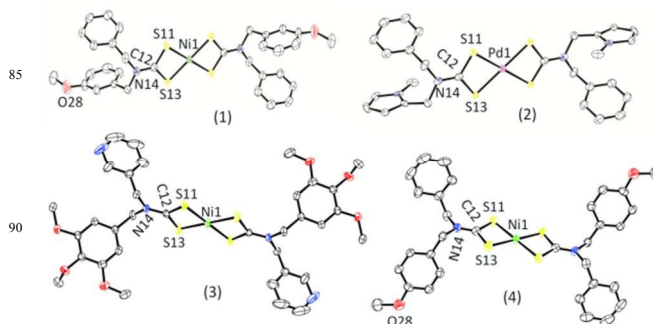


Fig. 3 ORTEP diagrams of **1-4** with displacement ellipsoids at 30% probability. Hydrogen atoms are omitted for clarity. In **1** the -OMe is disordered over the two *meta* sites: only one is shown. In **2**, the ligand is disordered with N-methyl-2-pyrrole and phenyl rings refined in

superimposed positions with 50% occupancy. The latter ring is not shown.

The basic structural features of all complexes are equivalent. The metal atom lies at the centre of a distorted square plane; the distortion varies, Pd greater than Ni. The distortion is caused due to small S(11)-M(1)-S(13) bite angles of 79.36(3), 79.39(4) and 79.60(4)° for M=Ni and 75.38(6)° for M=Pd. The Ni-S distances in the range 2.188(1) - 2.202(1) Å for **1**, **3** and **4** are shorter than the Pd-S distance of 2.321(2), 2.324(2) Å for **2**, values which are indicative of symmetrical (S,S) chelating behaviour of the dithiocarbamate ligands. The C(12)-N(14) bond lengths in the range 1.301(5)-1.316(8) Å are intermediate between the C-N (1.47 Å) and C=N (1.28 Å) bonds in accordance with the dominant contribution of the resonance form IV of Fig. 1. The C-S bond lengths of 1.711(7)-1.728(5) Å are considerably shorter than the C-S (1.81 Å) bond observed in the transition metal dithio complexes¹ due to π delocalisation over the NCS₂ unit. The chelating S₂CM rings with atoms S(11), C(12), S(13), M(1) are approximately coplanar in all the complexes. In all the complexes the supramolecular structures are sustained via O···H, N···H and S···H non-covalent interactions (Table 2) and additionally by C-H··· π (chelate, CS₂Ni) and/or C-H···Ni interactions^{9a} in **3** and **4**. Interestingly, the crystal packing in **1** and **2** oriented the C-H hydrogen atom of the methylene group on the benzyl and pyrrole substituents, in close proximity of the metal coordination sphere forming C-H···M (Ni, Pd) intermolecular anagostic or preagostic interactions generating 1-D polymeric chain motif. In both complexes the methylene hydrogen atoms occupy vacant axial sites at the metal centres establishing a pseudo octahedral coordination environment. The Ni···H-C distance and \angle Ni···H-C angle of 2.78 Å and 137° in **1** (Fig. 4 a, b) are well within the range for the anagostic interactions.¹⁰ In **2**, despite the larger size of palladium, the Pd···H-C distance of 2.61 Å is shorter than in the nickel complex and the \angle Pd···H-C angle of 173° is close to 180° (nearly linear) thus demonstrating the existence of spectacular C-H···Pd intermolecular electrostatic interactions which are on the borderline between the anagostic and hydrogen bonding interactions^{10f} (Fig. 4c, d) and do not persist in solution (*vide supra* synthesis and spectroscopy).

However by contrast in **3**, it is not clear whether the methylene hydrogen atom interacts more with the chelating NiS₂C dithiocarbamate ring or with the nickel atom. Distances from the centre of gravity (CG) of the ring and the metal atom are 3.61 and 3.24 Å respectively with \angle C-H···CG and \angle C-H···Ni angles of 153 and 133°. The \angle H···CG···Ni and \angle H···Ni···CG angles are 91 and 64° respectively. In **4**, the arrangement is clearer. Distances from the ring CG and the metal atom are 3.07 and 3.70 Å with C-H···CG and C-H···Ni angles of 137 and 134° and \angle H-CG-Ni and \angle H-Ni-CG angles of 102 and 54° respectively so that it is clear the interaction is with the ring^{9a} (Fig. 5), rather than the metal as is found in **1** and **2**. The nearest S···S intermolecular contacts between the coordinated dithiocarbamate ligands in **1-4** are in the 4.273-5.989 Å range which are significantly larger than are expected for prominent S···S intermolecular associations. It can therefore be noted that in **3** and **4** the benzyl methylene hydrogen atoms are not involved in the anagostic interactions with the metal rather the interaction is with the ring.

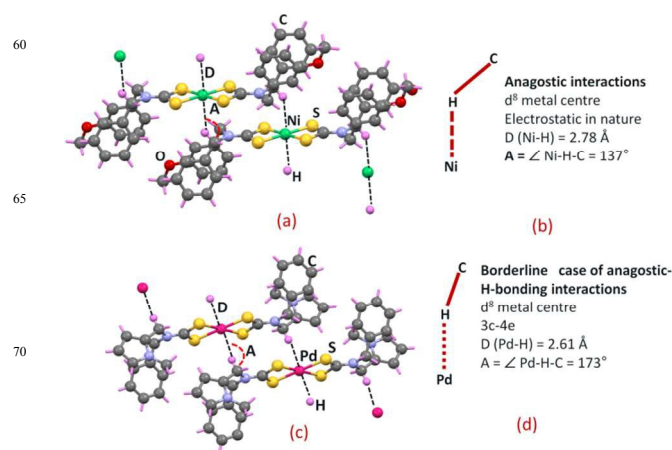


Fig. 4 (a), (b) Intermolecular C-H···M anagostic interactions with C-H···M distance (i.e. D) at 2.78 Å and \angle M···H-C (i.e. A) of 137° in **1**; (c), (d) Borderline case of anagostic-H-bonding interactions in **2**, D = 2.61 Å and A = 173°.

The steric hindrance due to bulkier 3,4,5-trimethoxy benzyl substituents in **3** probably resulted in the lack of such interactions but in **4** despite small steric bulk the methylene hydrogen atoms abstain from the anagostic interactions, a fact which may be ascribed to the crystal packing forces. Apparently, the incorporation of N-heteroaromatic functionalities such as 3-pyridyl in **3** and N-methyl pyrrole in **2** did not play any role in the generation of metal-assisted interactions. A further look into the molecular structures of **1-4** revealed that the orientation of aromatic rings is crucial for the proximity of the methylene hydrogen atoms to the metal centres. In **1** and **2** the aromatic rings face each other, placed almost one over the other while in **3** and **4** they are antagonistically placed thereby probably creating a less favourable orientation of the methylene hydrogen atoms in the vicinity of the metal centres (Fig. 3, 4). The CG-CG distance between the parallel rings in **1** and **2** are 3.79 and 4.09 Å respectively while those between the antagonistic rings in **3** and **4** at 5.71 and 6.20 Å are significantly larger.

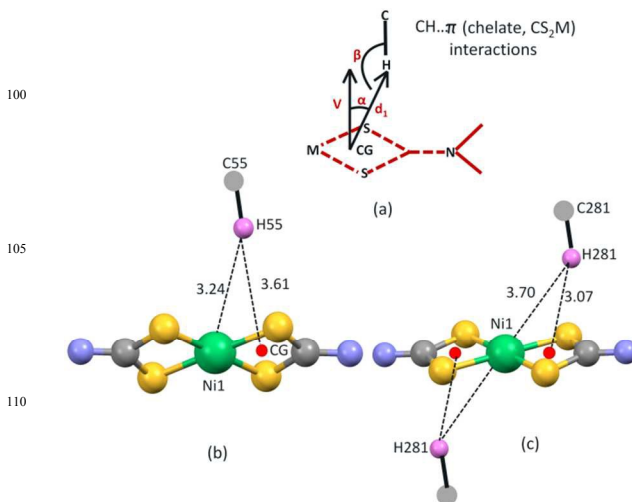


Fig. 5 (a) Generalized depiction of C-H··· π (chelate, CS₂M) interactions (b) Intermolecular C-H···CG and C-H···Ni interactions in (c) **3**, C-H···CG = 3.61 Å; C-H···Ni = 3.24 Å; \angle C-H···CG = 153°; \angle C-H···Ni = 133°

Cite this: DOI: 10.1039/c0xx00000x

www.rsc.org/xxxxxx

ARTICLE TYPE

= 133°; $\angle \text{H}\cdots\text{CG}\cdots\text{Ni} = 91^\circ$; $\angle \text{H}\cdots\text{Ni}\cdots\text{CG} = 64^\circ$ and (b) **4**, $\text{C-H}\cdots\text{CG} = 3.07 \text{ \AA}$; $\text{C-H}\cdots\text{Ni} = 3.70 \text{ \AA}$; $\angle \text{C-H}\cdots\text{CG} = 137^\circ$; $\angle \text{C-H}\cdots\text{Ni} = 134^\circ$; $\angle \text{H}\cdots\text{CG}\cdots\text{Ni} = 102^\circ$; $\angle \text{H}\cdots\text{Ni}\cdots\text{CG} = 54^\circ$.

From the DFT calculations it is possible to calculate the stabilisation energy of the packing due to $\text{C-H}\cdots\text{Ni/Pd}$ interactions. To eliminate the stabilization effect due to other secondary interactions in **1** and **2** (Table 2) some model compounds were designed. Thus the aromatic rings in the ligand moieties were replaced by methyl group (Fig. 6) and single point calculations were performed. The energy difference of $E(\text{trimer}) - 3 * E(\text{monomer})$ was -3.89 kcal/mol for **1** and -2.37 kcal/mol for **2**.^{11f} Thus, we can propose that these interactions are real anagostic / H-bonding interactions and affect the overall stability of the molecule in the supramolecular structure in the solid state. It seems likely that the presence of the $\text{M}\cdots\text{H}$ interaction is caused due to steric effects and favourable packing of the molecules which leads to the close contact between the metal and the methylene hydrogen atom.

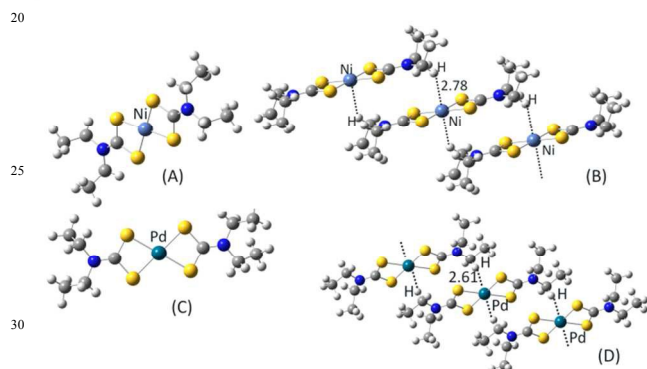


Fig. 6 Structure of model compounds used for assessing the $\text{C-H}\cdots\text{M}$ anagostic interactions in **1** (model A, B) and borderline anagostic-hydrogen bonding interactions in **2** (model C, D).

Table 1. Selected bond distances and angles for **1-4**

	Bonds (Å)			
	1 (M=Ni)	2 (M=Pd)	3 (M=Ni)	4 (M=Ni)
M(1)-S(11)	2.2006(7)	2.3213(16)	2.2070(10)	2.1904(12)
M(1)-S(13)	2.1932(7)	2.3239(16)	2.1875(10)	2.2024(13)
S(11)-C(12)	1.725(3)	1.711(7)	1.719(3)	1.728(5)
S(13)-C(12)	1.719(3)	1.731(6)	1.710(3)	1.727(4)
C(12)-N(14)	1.311(3)	1.316(8)	1.315(4)	1.301(5)
Bond angles (°)				
S(11)-M(1)-S(13)	79.36(3)	75.38(6)	79.39(4)	79.60(4)
M(1)-S(11)-C(12)	85.57(9)	87.0(2)	84.93(12)	85.87(16)
M(1)-S(13)-C(12)	85.96(9)	86.4(2)	85.74(11)	85.51(16)
S(11)-C(12)-S(13)	109.09(14)	111.2(4)	109.88(19)	108.9(3)

Table 2. Weak secondary interactions and their vital parameters observed in compounds **1-4**

Compound code	D-H...A	d(H...A) (Å)	d(D...A) (Å)	$\angle \text{D-H}\cdots\text{A}$ (°)
1	C24-H24...O28	2.44	3.36	174
	C34-H38...O24	2.50	3.26	139
2	C37A-H37C...S13	2.94	3.88	166
	C251-H25B...O24	2.47	3.42	171
3	C241-H24A...N56	2.70	3.28	120
	C281-H281...S13	2.78	3.72	165
4	C23-H23...O28	2.63	3.30	129
Symmetry code: 1. $-1+x,y,z$ 2. $x,-1+y,z$ 3. $-3+x,1+y,-1+z$; $x,1+y,z$ 4. $-1/2-x,-1/2+y,1$; $2-z$; $-1/2-x,-1/2+y,-1/2-z$				

Absorption spectra

The electronic absorption spectra of **1-4** in dichloromethane solution (Fig. S1, ESI) show bands near 241-247 ($\epsilon = 1.9 \times 10^5 - 3.9 \times 10^4 \text{ M}^{-1}\text{cm}^{-1}$), 300-330 ($\epsilon = 1.6 \times 10^5 - 7.8 \times 10^4 \text{ M}^{-1}\text{cm}^{-1}$), 355-450 ($\epsilon = 1.6 \times 10^4 - 1.3 \times 10^3$) and 632-635 nm ($\epsilon = 114 - 167 \text{ M}^{-1}\text{cm}^{-1}$) assignable to intraligand charge transfer (ILCT), ligand (S) to metal charge transfer (LMCT) and d-d transitions respectively consistent with square planar geometry¹⁷ about the metal centre. In the case of the Pd complex **2**, the d-d band is not observed.

Pressed Pellet Conductivity

Pressed pellet electrical conductivity of **1**, **3** and **4** was measured with a Keithly 236 source measure unit by employing the conventional two-probe technique. All the complexes are weakly conducting at room temperature ($\sigma_{\text{rt}} = 10^{-10} - 10^{-12} \text{ S cm}^{-1}$, $E_a = 1.44 - 1.55 \text{ eV}$) but they show semiconductor property^{3d,e} in the 313-373 K temperature range as their conductivity increases with increasing temperature (Fig. S2, ESI) and decreases with decrease in temperature. The weakly conducting nature of the complexes may be attributed to the lack of efficient $\text{S}\cdots\text{S}$ intermolecular interactions in the solid state (*vide supra* X-ray structures).

Conclusions

Among new functionalized homoleptic Ni(II) and Pd(II) dithiocarbamate complexes (**1-4**), the X-ray crystallography revealed the existence of interesting intermolecular $\text{C-H}\cdots\text{M}$ (Ni, Pd) anagostic interactions generating 1-D polymeric chain motifs perforce by crystal packing in **1** and **2**. The geometric parameters revealed that the $\text{C-H}\cdots\text{Pd}$ interactions in **2** are on the borderline between anagostic and hydrogen bonding interactions. In these structures the vacant axial sites on the metal centres are occupied by the methylene hydrogen atoms on the ligand fragments thereby providing pseudo octahedral environments. However in **3** and **4**, the interactions of the methylene hydrogen atom are subtly different. In **4** the prime interaction is with the NiS_2C ring rather than the metal, while in **3** the interaction is intermediate between the two aforementioned types with the centre of gravity of the ring and

the metal. These types of bonding interactions involving the metal centres are of considerable importance in the transition metals as well as main group chemistry due to their possible involvement in the C-H bond activation in the organic synthesis. Complex **1** having a methoxy group at the meta-
 5 position of benzene ring exhibits anagostic interactions while **4** having methoxy group at the para-position does not possess any such interactions. The former has overlapping aromatic rings of the functionalities (a feature also observed in **2**) while

the latter has the rings antagonistically placed. This may be a contributing factor in the favourable orientation of the methylene hydrogen atoms for the generation of these interactions. This study demonstrates that the crystal packing forces significantly influence the construction of metal assisted
 15 C-H intermolecular interactions rather than the functionalities on the N atom of the dithiocarbamate backbone in these complexes.

Table 3. Crystal data and refinement parameters

Compound	1	2	3	4
Chemical Formula	C ₃₂ H ₃₂ N ₂ NiO ₂ S ₄	C ₂₉ H ₂₉ N ₃ PdS ₄	C ₃₄ H ₃₈ N ₄ NiO ₆ S ₄	C ₃₂ H ₃₂ N ₂ NiO ₂ S ₄
Formula Weight	663.55	654.19	785.63	663.55
Crystal system	triclinic	triclinic	triclinic	monoclinic
Space group	P-1	P-1	P-1	P21/n
<i>a</i> (Å)	6.4945(7)	6.7086(10)	7.0268(10)	8.3049(6)
<i>b</i> (Å)	11.1068(10)	10.3187(18)	10.6267(18)	21.4036(11)
<i>c</i> (Å)	11.7301(13)	10.8136(12)	13.7577(16)	9.1470(7)
α (°)	101.467(9)	74.967(12)	104.768(12)	(90)
β (°)	102.098(9)	84.813(10)	103.014(11)	103.09(7)
γ (°)	106.947(9)	72.281(14)	105.644(14)	(90)
<i>V</i> (Å ³)	760.24(14)	688.59(18)	907.7(2)	1580.27(19)
<i>Z</i>	1	1	1	2
ρ_{calc} (g cm ⁻³)	1.449	1.578	1.437	1.394
T(K)	293(2)	150(2)	293(2)	293(2)
μ (Mo K α) (mm ⁻¹)	0.946	1.002	0.814	0.910
<i>F</i> (000)	346	334	410	692
Reflections collected	5443	4823	6893	7133
Independent reflns	3340	3838	3961	3467
Reflections with <i>I</i> >2 σ (<i>I</i>)	2509	2704	2465	1927
Final indices [<i>I</i> >2 σ (<i>I</i>)]	0.0431, 0.1045	0.0931, 0.2176	0.0523, 0.1103	0.0740, 0.1471
<i>R</i> ₁ ^a , w <i>R</i> ₂ ^b				
<i>R</i> ₁ ^a , w <i>R</i> ₂ ^b [all data]	0.0629, 0.1142	0.1217, 0.2487	0.1042, 0.1286	0.1422, 0.1741
GOF	0.964	1.022	0.986	1.013
CCDC number	1014554	1014555	1014556	1014557

^a $R_1 = \sum ||F_o| - |F_c|| / \sum |F_o|$. ^b $R_2 = \{[\sum w(F_o^2 - F_c^2)^2] / \sum w(F_o^2)^2\}^{1/2}$, $w = 1/[\sigma^2(F_o^2) + (xP)^2]$, where $P = (F_o^2 + 2F_c^2)/3$

Acknowledgements

We gratefully acknowledge the Council of Scientific and Industrial research (CSIR), New Delhi, for SRF (GR) and Project
 25 No. 01 (2679)/12/EMR-II (NS, MKY) and the Department of Chemistry, Banaras Hindu University, Varanasi for X-ray diffraction facility.

Notes and references

^a Department of Chemistry, Faculty of Science, Banaras Hindu
 30 University,

Varanasi 221005, India. Fax: +91-542-2386127

E-mail: nsingh@bhu.ac.in, nsinghbhu@gmail.com

^b Department of Chemistry, University of Reading, Whiteknights,
 Reading, RG6 6AD (U.K.)

[†] Electronic Supplementary Information (ESI) available: [Figure for
 35 absorption spectra and pressed pellet conductivity of 1-4]. See
 DOI: 10.1039/b000000x/

- (a) D. Coucouvanis, *Prog. Inorg. Chem.*, 1979, **26**, 301; (b) G. Hogarth, *Prog. Inorg. Chem.*, 2005, **53**, 71; (c) J. Cookson and P. D. Beer, *Dalton Trans.*, 2007, **15**, 1459; (d) P. J. Heard, *Prog. Inorg. Chem.*, 2005, **53**, 268.
- (a) J. D. E. T. Wilton-Ely, D. Solanki, E. R. Knight, K. B. Holt, A. L. Thompson and G. Hogarth, *Inorg. Chem.*, 2008, **47**, 9642; (b) G. Hogarth, E.-J. C.-R. Rainford-Bent, S. E. Kabir, I. Richards, J.D. E. T. Wilton-Ely and Qi Zhang, *Inorg. Chim. Acta*, 2009, **362**, 2020.
- (a) E. R. T. Tiekink and I. Haiduc, *Prog. Inorg. Chem.*, 2005, **54**, 127; (b) C. S. Lai and E. R. T. Tiekink, *CrystEngComm*, 2003, **5**, 253; (c) T. Okubo, N. Tanaka, K. H. Kim, H. Yone, M. Maekawa and T. Kuroda-Sowa, *Inorg. Chem.*, 2010, **49**, 3700; (d) T. Okubo, H. Anma, N. Tanaka, K. Himoto, S. Seki, A. Saeki, M. Maekawa and T. Kuroda-Sowa, *Chem. Commun.*, 2013, **49**, 4316; (e) P. I. Clemenson, *Coord. Chem. Rev.*, 1990, **106**, 171.
- (a) E. J. Mensforth, M. R. Hill and S. R. Batten, *Inorg. Chim. Acta*, 2013, **403**, 9; (b) S. Naeem, S. A. Serapian, A. Toscani, A. J. P. White, G. Hogarth and J. D. E. T. Wilton-Ely, *Inorg. Chem.*, 2014, **53**, 2404.

- 5 (a) M. Bousseau, L. Valade, J. P. Legros, P. Cassoux, M. Garboukas and L. V. Interrante, *J. Am. Chem. Soc.*, 1986, **108**, 1908; (b) P. Cassoux and L. Valade, *Inorganic Materials*, John Wiley and Sons, Chichester, 1996.
- 5 6 (a) A. Kumar, R. Chauhan, K. C. Molloy, G. Kociok-Kohn, L. Bahadur and N. Singh, *Chem. Eur. J.*, 2010, **16**, 4307; (b) G. Rajput, V. Singh, S. K. Singh, L. B. Prasad, M. G. B. Drew, N. Singh, *Eur. J. Inorg. Chem.*, 2012, **24**, 3885; (c) V. Singh, R. Chauhan, A. Kumar, L. Bahadur and N. Singh, *Dalton Trans.*, 2010, **39**, 9779; (d) V. Singh, A. Kumar, R. Prasad, G. Rajput and N. Singh, *CrystEngComm*, 2011, **13**, 6817; (e) R. Angamuthu, L. L. Gelauuff, M. A. Siegler, A. L. Spek and E. Bouwman, *Chem. Commun.*, 2009, **19**, 2700; (f) V. Singh, R. Chauhan, A. N. Gupta, V. Kumar, M. G. B. Drew, N. Singh, *Dalton Trans.*, 2014, **43**, 4752; (g) S. K. Singh, M. G. B. Drew and N. Singh, *CrystEngComm*, 2013, **15**, 10255; (h) B. Singh, M. G. B. Drew, G. Kociok-Kohn, K. C. Molloy and N. Singh, *Dalton Trans.*, 2011, **40**, 623; (i) G. Rajput, V. Singh, A. N. Gupta, M. K. Yadav, V. Kumar, S. K. Singh, A. Prasad, M. G. B. Drew and N. Singh, *CrystEngComm*, 2013, **15**, 4676; (j) E. A. M. Geary, N. Hirata, J. Clifford, J. R. Durrant, S. Parsons, A. Dawson, L. J. Yellowlees and N. Robertson, *Dalton Trans.*, 2003, **19**, 3757.
- 7 (a) P. O' Brien and J. H. Park and J. Waters, *Thin. Solid. Films*, 2003, **431**, 502; (b) P. O' Brien and J. Waters, *Chem. Vap. Deposition*, 2006, **12**, 1208; (c) N. Alam, M. S. Hill, G. Kociok-Kohn, M. Zeller, M. Mazhar and K. C. Molloy, *Chem. Mater.*, 2008, **20**, 6157; (d) M. S. Vickers, J. Cookson, P. D. Beer, P. T. Bishop and B. Thiebaut, *J. Mater. Chem.*, 2006, **16**, 209.
- 8 (a) G. R. Desiraju, *Chem. Commun.*, 2005, **24**, 2995; (b) C. R. Kaiser, K. C. Pais, M. V. N. de Souza, J. L. Wardell, S. M. S. V. Wardell and E. R. T. Tiekink, *CrystEngComm*, 2009, **11**, 1133; (b) Y. R. Zhong, M. L. Cao, H. J. Mo and B. H. Ye, *Cryst. Growth Des.*, 2008, **8**, 2282; (c) S. Takahashi, T. Jukurogi, T. Katagiri and K. Uneyama, *CrystEngComm*, 2006, **8**, 320; (d) A. N. Sokolov, T. Friscic, S. Blais, J. A. Ripmeester and L. R. MacGillivray, *Cryst. Growth Des.*, 2006, **6**, 2427; (e) J. W. Steed and J. L. Atwood, *Supramolecular Chemistry*, VCH, New York, 2000. (f) D. R. Armstrong, M. G. Davidson and D. Moncrief, *Angew. Chem., Int. Ed. Engl.*, 1995, **34**, 478.
- 9 (a) E. R. T. Tiekink and J-Z. Schpector, *J. Chem. Soc. Chem. Commun.*, 2011, **47**, 6623; (b) P. W.G. Newman and A. H. White, *J. Chem. Soc. Dalton Trans.*, 1972, **14**, 1460; (c) P. W.G. Newman and A. H. White, *J.C.S. Dalton Trans.*, 1972, **20**, 2239; (d) J. W. Martin, P. W. G. Newman, B. W. Robinson and A. H. White, *J. C. S. Dalton Trans.*, 1972, **20**, 2233.
- 10 (a) M. Brookhart, M. L. H. Green and G. Parkin, *Proc. Natl. Acad. Sci. U. S. A.*, 2007, **104**, 6908; (b) H. V. Huynh, L. R. Wong and P. S. Ng, *Organometallics*, 2008, **27**, 2231; (c) W. Yao, O. Eisenstein and R. H. Crabtree, *Inorg. Chim. Acta*, 1997, **254**, 105; (d) J. Saßmannshausen, *Dalton Trans.*, 2012, **41**, 1919; (e) Y. Zhang, J. C. Lewis, R. G. Bergman, J. A. Ellman and E. Oldfield, *Organometallics*, 2006, **25**, 3515; (f) K. A. Siddiqui and E. R. T. Tiekink, *Chem. Commun.*, 2013, **49**, 8501; (g) S. Schöler, M. H. Wahl, N. I. C. Wurster, A. Puls, C. Hättig, G. Dyker, *Chem. Commun.*, 2014, **50**, 5909; (h) M. G. D. Holaday, G. Tarafdar, A. Kumar, M. L. P. Reddy and A. Srinivasan, *Dalton Trans.*, 2014, **43**, 7699.
- 11 (a) L. Brammer, *Dalton Trans.*, 2003, **16**, 3145; (b) E.S. Tabei, H. Samouei and M. Rashidi, *Dalton Trans.*, 2011, **40**, 11385; (c) J. C. Lewis, J. Wu, R. G. Bergman and J. A. Ellman, *Organometallics*, 2005, **24**, 5737; (d) D. Braga, F. Grepioni, E. Tedesco, K. Biradha, G. R. Desiraju, *Organometallics*, 1997, **16**, 1846; (e) S. Rizzato, J. Berges, S. A. Mason, A. Albinati and J. Kozelka, *Angew. Chem., Int. Ed.*, 2010, **49**, 7440.
- 70 12 (a) M. Baya, U. Belio, A. Martin, *Inorg. Chem.*, 2014, **53**, 189-200; (b) F. Kraus, H. Schmidbaur, S. S. Al-juaid, *Inorg. Chem.*, 2013, **52**, 9669-9674; (c) E. M. Barranco, O. Crespo, M. C. Gimeno, P. G. Jones and A. Laguna, *Eur. J. Inorg. Chem.*, 2004, **24**, 4820.
- 75 13 Oxford Diffraction, CrysAlis CCD, RED, version 1.711.13, copyright 1995–2003, Oxford Diffraction Poland Sp.
- 14 G. M. Sheldrick, *Acta Crystallogr.*, 2008, **A64**, 112.
- 15 M. N. Burnett and C. K. Johnson, ORTEP-III, Oak Ridge Thermal Ellipsoid Plot Program for Crystal Structure Illustrations, Report ORNL-6895, Oak Ridge National Laboratory, Oak Ridge, TN, USA, 1996.
- 80 16 M.J. Frisch, G. W. Trucks, H. B. Schlegel, G. E. Scuseria, M. A. Robb, J. R. Cheeseman, J. A. Montgomery, T. Vreven, K. N. Kudin, J. C. Burant, J. M. Millam, S. S. Iyengar, J. Tomasi, V. Barone, B. Mennucci, M. Cossi, G. Scalmani, N. Rega, G. A. Petersson, H. Nakatsuji, M. Hada, M. Ehara, K. Toyota, R. Fukuda, J. Hasegawa, M. Ishida, T. Nakajima, Y. Honda, O. Kitao, H. Nakai, M. Klene, X. Li, J. E. Knox, H. P. Hratchian, J. B. Cross, V. Bakken, C. Adamo, J. Jaramillo, R. Gomperts, R. E. Stratmann, O. Yazyev, A. J. Austin, R. Cammi, C. Pomelli, J. W. Ochterski, P. Y. Ayala, K. Morokuma, G. A. Voth, P. Salvador, J. J. Dannenberg, V. G. Zakrzewski, S. Dapprich, A. D. Daniels, M. C. Strain, O. Farkas, D. K. Malick, A. D. Rabuck, K. Raghavachari, J. B. Foresman, J. V. Ortiz, Q. Cui, A. G. Baboul, S. Clifford, J. Cioslowski, B. B. Stefanov, G. Liu, A. Liashenko, P. Piskorz, I. Komaromi, R. L. Martin, D. J. Fox, T. Keith, M. A. Al-Laham, C. Y. Peng, A. Nanayakkara, M. Challacombe, P. M. W. Gill, B. Johnson, W. Chen, M. W. Wong, C. Gonzalez and J. A. Pople, *Gaussian 03*, revision C.02; Gaussian, Inc.: Wallingford, CT, U.S.A.
- 90 17 A. B. P. Lever, *Inorganic Electronic Spectroscopy*, Elsevier, Amsterdam, 1984.